International Journal of Thermofluid Science and Technology (2021)
Volume 8, Issue 1, Paper No. 080104
https://doi.org/10.36963/IJTST.2021080104
Research Article

Combined effects of nonuniform temperature gradients and heat source on double diffusive Benard-Marangoni convection in a porous-fluid system in the presence of vertical magnetic field

Manjunatha N[1], Sumithra R[2], Vanishree R K[3]

[1]*Department of Mathematics, School of Applied Sciences, REVA University, Bengaluru-560064, India*
[2]*Department of UG, PG Studies & Research in Mathematics, Government Science College Autonomous, Bengaluru-560001, India*
[3]*Department of Mathematics, Maharani's Science College for Women, Maharani's Cluster University, Bengaluru-560001, India*

Received: 15 December 2020; Received in revised form: 25 January 2021; Accepted: 25 February 2020; Published online 10 March 2021

Abstract

The physical configuration of the problem is a porous-fluid layer which is horizontally unbounded, in the presence of uniform heat source/sink in the layers enclosed by adiabatic and isothermal boundaries. The problem of double diffusive Bènard-Marangoni convection in the presence of vertical magnetic field is investigated on this porous-fluid system for non-Darcian case and is subjected to uniform and nonuniform temperature gradients. The eigenvalue, thermal Marangoni number is obtained in the closed form for lower rigid and upper free with surface tension velocity boundary conditions. The influence of various parameters on the Marangoni number against thermal ratio is discussed. It is observed that the heat absorption in the fluid layer and the applied magnetic field play an important role in controlling Benard-Marangoni convection. The parameters which direct this convection are determined and the effect of porous parameter is relatively interesting.

Keywords: Benard-Marangoni convection, Heat source, Thermal ratio, Magnetic field, Temperature gradients, porous-fluid system, Adiabatic & isothermal boundaries.

1. Introduction

Double diffusion is a phenomenon which describes the transportation that occurs within a system containing a fluid with two diffusing components. The buoyancy force in the fluid that may initiate the motion is due to the gradients of these diffusing components. Double diffusive convection is very important to understand the evolution of system that has different causes for density variations. Some of them are convection in earth's mantle, oceans and in the sun. It is considered to be important below the sediment laden rivers in lakes and the ocean. Thermal and chemical interactions in a composite layer (fluid overlying a porous

Corresponding e-mail: manjunatha.n@reva.edu.in (Manjunatha N)

layer) find wide range of applications in chemical engineering, oceanography, geophysics, thermal engineering. Double diffusive convection in a composite layer has several applications such as soil pollution, thermal insulation, grain storage, dispersion of chemical contaminants through the water saturated soil, storage of nuclear waste, fuel cells, heat removal from nuclear fuel debris in nuclear reactors, thermal energy storage system, solar collectors with a porous absorber etc. One more important application lies in modeling the boundary conditions at the interface. Due to its theoretical importance in understanding the interface boundary conditions and practical interests as listed above, this problem has been researched intensively by many researchers. Sumithra and Manjunatha [1] examined the effects of parabolic and inverted parabolic on composite layer and obtained the closed form of solution for thermal Marangoni number. Numerical study of double-diffusive convection developed within horizontal partially porous enclosure studied by Noureddine Hadidi et al. [2]. Manjunatha and Sumithra [3] studied the effects of non-uniform temperature gradients on double diffusive Marangoni convection in a two layer system. Magnetic field effect on double diffusive convection in an electrically conducting viscoelastic fluid saturated porous layer in the presence of internal heat source is studied analytically using linear stability analysis by Altawallbeh et al. [4]. Sumithra et al. [5] discussed the Darcy-Benard double diffusive Marangoni convection with Soret effect in a composite layer system using exact technique.

Marangoni (surface tension driven) convection, also called Benard-Marangoni convection has been well understood and documented by several researchers. The stability analysis of Marangoni convection in porous media with a deformable upper free surface is investigated by Mokhtar et al. [6]. The effects of thermal anisotropy and mechanical anisotropy on the onset of Bernard-Marangoni convection in composite layers with anisotropic porous material is studied by Gangadharaiah [7]. Controlling of convection is an important application in many industrial applications. A heat source (sink) of constant strength can be effectively used to augment/delay the convection. Mehmood et al. [8] studied the effect of a non-uniform heat source/sink in a thermally and solutally stratified magneto nanofluid using RK4 method with shooting technique. Effects of heat source/sink and induced magnetic field on the natural convective flow in vertical concentric annuli studied by Dileep Kumar and Singh [9]. Effects of heat source/sink and chemical reaction to MHD Maxwell nanofluid flow over a convectively heated exponentially stretching sheet by Sravanthi and Gorla [10] using the Homotopy analysis method. Radiation and non-uniform heat sink/source effects on 2D MHD flows of CNTs- H_2O nanofluid over a flat porous plate studied by Upreti et al. [11]. The effect of temperature-dependent viscosity in a horizontal double diffusive binary fluid layer is investigated by Nurul Hafizah Zainal Abidin et al. [12]. They found that the effect of the Soret parameter exhibits destabilizing reaction on the system while an opposite response is noted with an increase of Dufour parameter. The impact of non-uniform heat source/sink and temperature dependent viscosity modeled by Reynolds on Cattaneo-Christov heat flow of third grade nanofluid subject to an inclined stretched Riga plate by Nayak et al. [13] using fourth order R-K and shooting methods.

Recently, Nadeem et al. [14] studied Darcy-Forchheimer flow under rotating disk and entropy generation with thermal radiation and heat source/sink. They noticed from the present analysis that the irreversibility rate and Bejan number have reverse behavior for Brinkmann number. Thirupathi Thumma and Mishra [15] studied the effect of nonuniform

heat source/sink, and viscous and Joule dissipation on 3D Eyring-Powell nanofluid flow over a stretching sheet using the Adomian decomposition method. Ali J. Chamkha et al. [16] used numerical analysis to investigate the importance of hybrid nanofluid in the free convection inside a partially heated square cavity and subjected to the inclined magnetic field with heat generation/absorption. Talha Anwar et al. [17] investigated a comprehensive analysis of time-dependent free convection electrically and thermally conducted water-based nanofluid flow containing Copper and Titanium oxide past a moving porous vertical plate. Mandal and Mukhopadhyay [18] studied the nonlinear convection in micropolar fluid flow past a non-isothermal exponentially permeable stretching sheet in the presence of heat source/sink with the help of shooting technique and Runge-Kutta method. Presence of magnetic field also can be effectively used to regulate convection. Dharmaiah et al. [19] studied the Perturbation analysis of thermophoresis, hall current and heat source on flow dissipative aligned convective flow about an inclined plate. Tarikul Islam et al. [20] studied the free convection flow and temperature transfer within a right-angled triangular cavity loaded uniformly by Cu-H_2O nanofluid including heated boundary conditions at horizontal side is performed numerically. Manjunatha and Sumithra [21, 22] and Vanishree et al. [23] studied the effect of constant heat source / sink and temperature gradients on composite layer with and without magnetic field. They obtained the closed form of solution to thermal Marangoni number for three different temperature gradients.

Owing to its importance in understanding many naturally occurring/industry related situations, in this paper, double diffusive Bènard-Marangoni convection in a composite layer in the presence of heat source (sink) with temperature gradients under the influence of a magnetic field for a sparsely packed porous medium is considered.

Nomenclature

A ratio of heat capacities	T_0 interface temperature
a , a_m horizontal wave numbers	$\vec{V}$ velocity vector
C concentration	$W(z)$ vertical velocity in fluid layer
C_0 interface concentration	$W_m(z_m)$ vertical velocity in porous layer
$\hat{d}$ depth ratio	ρ_0 Fluid density
K permeability of the porous medium	β Porous parameter
M_s solute Marangoni number	ε porosity
M_t thermal Marangoni number	κ thermal diffusivity of the fluid
P pressure	κ_c solute diffusivity of the fluid
R_I^* modified internal Rayleigh number for fluid region	μ fluid viscosity
R_i internal Rayleigh number for fluid region	μ_m effective viscosity of the fluid in the porous layer
R_{Im}^* modified internal Rayleigh number for porous region	$\hat{\mu}$ viscosity ratio
R_{im} internal Rayleigh number for porous region	τ diffusivity ratio for fluid layer

$S(z)$ concentration distribution in fluid layer	τ_{pm} diffusivity ratio for porous layer
$S_m(z_m)$ concentration distribution in porous layer	σ_t Surface tension
T temperature	$\theta(z)$ temperature distribution in fluid layer
$\hat{T}$ thermal ratio	$\theta_m(z_m)$ temperature distribution in porous layer

2. Formulation of the problem

In the current study, we consider a horizontal double component, electrically conducting fluid saturated isotropic, incompressible sparsely packed porous layer of thickness d_m underlying a two component fluid layer of thickness d with an imposed magnetic field intensity H_0 in the vertical z-direction and with heat sources Φ_m and Φ respectively. The lower surface of the porous layer rigid and the upper surface of the fluid layer is free with surface tension effects depending on temperature and concentration. A Cartesian coordinate system is chosen with the origin at the interface between porous and fluid layers and the z-axis, vertically upwards (Fig.1).

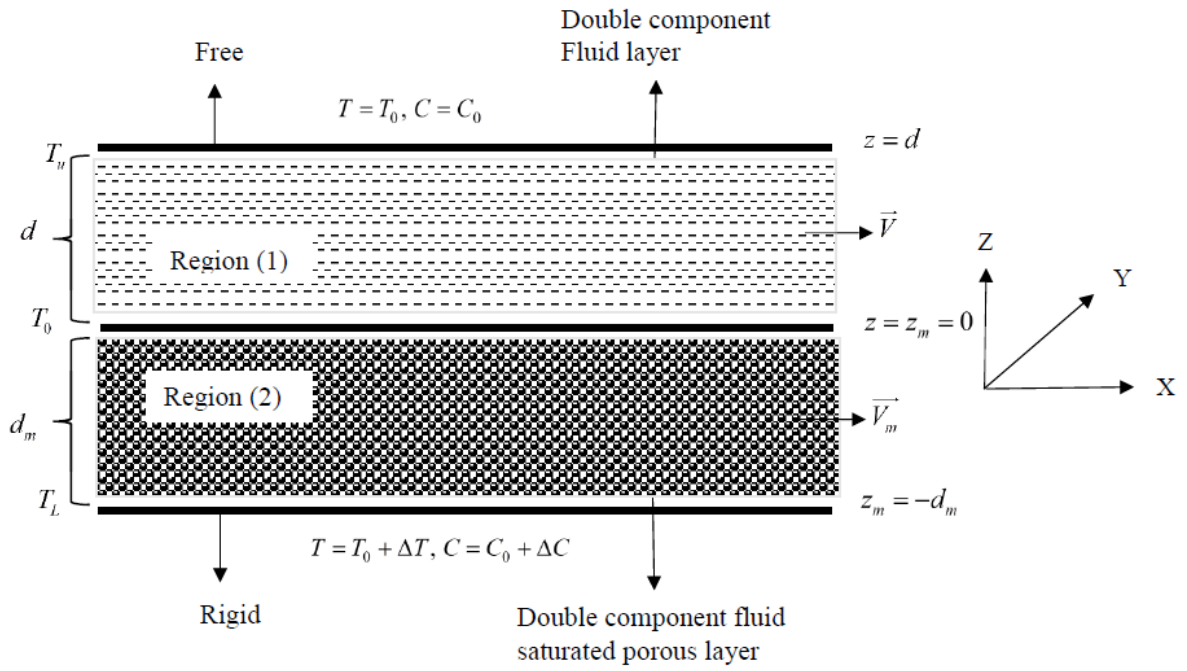

Fig. 1. Physical configuration of the system

The basic equations for fluid and porous layer respectively governing such a system are [1, 3, 21, 22, 24]:

$$\nabla.\vec{V} = 0 \tag{1}$$

$$\nabla.\vec{H} = 0 \tag{2}$$

$$\rho_0\left[\frac{\partial \vec{V}}{\partial t}+(\vec{V}.\nabla)\vec{V}\right]=-\nabla P+\mu\nabla^2\vec{V}+\mu_p(\vec{H}.\nabla)\vec{H} \tag{3}$$

$$\frac{\partial T}{\partial t}+(\vec{V}.\nabla)T=\kappa\nabla^2 T+\Phi \tag{4}$$

$$\frac{\partial C}{\partial t}+(\vec{V}.\nabla)C=\kappa_c\nabla^2 C \tag{5}$$

$$\frac{\partial \vec{H}}{\partial t}=\nabla\times\vec{V}\times\vec{H}+\nu\nabla^2\vec{H} \tag{6}$$

$$\nabla_m.\overrightarrow{V_m}=0 \tag{7}$$

$$\nabla_m.\vec{H}=0 \tag{8}$$

$$\rho_0\left[\frac{1}{\varepsilon}\frac{\partial \overrightarrow{V_m}}{\partial t}+\frac{1}{\varepsilon^2}(\overrightarrow{V_m}.\nabla_m)\overrightarrow{V_m}\right]=-\nabla_m P_m-\frac{\mu}{K}\overrightarrow{V_m}+\mu_m\nabla_m\overrightarrow{V_m}+\mu_p(\vec{H}.\nabla_m)\vec{H} \tag{9}$$

$$A\frac{\partial T_m}{\partial t}+(\overrightarrow{V_m}.\nabla_m)T_m=\kappa_m\nabla_m^2 T_m+\Phi_m \tag{10}$$

$$\varepsilon\frac{\partial C_m}{\partial t}+(\overrightarrow{V_m}.\nabla_m)C_m=\kappa_{cm}\nabla_m^2 C_m \tag{11}$$

$$\varepsilon\frac{\partial \vec{H}}{\partial t}=\nabla_m\times\overrightarrow{V_m}\times\vec{H}+\nu_{em}\nabla_m^2\vec{H} \tag{12}$$

where for fluid layer, $\vec{V}$ is the velocity vector, ρ_0 is the fluid density, t is time, μ is fluid viscosity, P is the total pressure, $\vec{H}$ is the magnetic field, T is temperature, κ is the thermal diffusivity of the fluid, ν is the magnetic viscosity and μ_p is the magnetic permeability. For porous layer, ε is the porosity, μ_m is the effective viscosity of the fluid in the porous layer, K is the permeability of the porous medium, A is the ratio of heat capacities, κ_m is the thermal diffusivity, ν_{em} is the effective magnetic viscosity and the subscript 'm' denotes the quantities in porous layer.

The aim of this paper is to investigate the stability of a quiescent state to infinitesimal perturbations superposed on the basic state.

The basic state is quiescent, have the following solutions,

Fluid layer:

$$\vec{V}=0, P=P_b(z), T=T_b(z), C=C_b(z), \vec{H}=H_0(z) \tag{13}$$

Porous layer:

$$\overrightarrow{V_m}=0, P_m=P_{mb}(z_m), T_m=T_{mb}(z_m), C_m=C_{mb}(z_m), \vec{H}=H_0(z_m) \tag{14}$$

The temperature distributions in the basic state are obtained by

$$T_b(z) = \frac{-\Phi z(z-d)}{2\kappa} + \frac{(T_u - T_0) f(z)}{d} + T_0 \quad in \quad 0 \le z \le d \tag{15}$$

$$T_{mb}(z_m) = \frac{-\Phi_m z_m (z_m + d_m)}{2\kappa_m} + \frac{(T_0 - T_l) f_m(z_m)}{d_m} + T_0 \quad in \quad -d_m \le z_m \le 0 \tag{16}$$

The concentration distributions in the basic state are obtained by

$$C_b(z) = C_0 - \frac{(C_0 - C_u) z}{d} \quad in \quad 0 \le z \le d \tag{17}$$

$$C_{mb}(z_m) = C_0 - \frac{(C_l - C_0) z_m}{d_m} \quad in \quad -d_m \le z_m \le 0 \tag{18}$$

where $T_0 = \frac{\kappa d_m T_u + \kappa_m d T_l}{\kappa d_m + \kappa_m d} + \frac{d d_m (\Phi_m d_m + \Phi d)}{2(\kappa d_m + \kappa_m d)}$, $C_0 = \frac{\kappa_c d_m C_u + \kappa_{cm} d C_l}{\kappa_c d_m + \kappa_{cm} d}$ are the interface temperature and concentration, $f(z)$ & $f_m(z_m)$ are the temperature gradients in fluid & porous layer respectively.

To investigate the stability of the basic state, infinitesimal disturbances are superimposed on fluid and porous layer respectively

$$\vec{V} = \vec{V}', P = P_b + P', T = T_b(z) + \theta, C = C_b(z) + S, \vec{H} = H_0(z) + \vec{H}' \tag{19}$$

$$\overrightarrow{V_m} = \overrightarrow{V_m}', P_m = P_{mb} + P_{m'}, T_m = T_{mb}(z_m) + \theta_m, C_m = C_{mb}(z_m) + S_m, \vec{H} = H_0(z_m) + \vec{H}' \tag{20}$$

Following the standard linear stability analysis procedure (Manjunatha and Sumithra [3, 21]) and assuming that the principle of exchange of stability holds, we arrive at the following stability equations:

in $0 \le z \le 1$

$$(D^2 - a^2)^2 W(z) = Q D^2 W(z) \tag{21}$$

$$(D^2 - a^2)\theta(z) + [f(z) + R_I^*(2z-1)]W(z) = 0 \tag{22}$$

$$\tau(D^2 - a^2)S(z) + W(z) = 0 \tag{23}$$

in $-1 \le z_m \le 0$

$$[(D_m^2 - a_m^2)\hat{\mu}\beta^2 - 1](D_m^2 - a_m^2)W_m(z_m) = Q_m \beta^2 D_m^2 W_m(z_m) \tag{24}$$

$$(D_m^2 - a_m^2)\theta_m(z_m) + [f_m(z_m) + R_{Im}^*(2z_m + 1)]W_m(z_m) = 0 \tag{25}$$

$$\tau_m(D_m^2 - a_m^2)S_m(z_m) + W_m(z_m) = 0 \tag{26}$$

In the above equations Q, $R_I^* = \frac{R_i}{2(T_0 - T_u)}$, $R_i = \frac{\Phi d^2}{\kappa}$, $\tau = \frac{\kappa_c}{\kappa}$ are namely, the Chandrasekhar number, the modified internal Rayleigh number, the internal Rayleigh number, the diffusivity ratio respectively for fluid layer and $\hat{\mu} = \frac{\mu_m}{\mu}$, $\beta = \sqrt{\frac{K}{d_m^2}}$, Q_m, $R_{Im}^* = \frac{R_{im}}{2(T_l - T_0)}$,

$R_{im} = \frac{\Phi_m d_m^2}{\kappa_m}$, $\tau_m = \frac{\kappa_{cm}}{\kappa_m}$ are namely, the viscosity ratio, the porous parameter, the Chandrasekhar number, the modified internal Rayleigh number, the internal Rayleigh number and the diffusivity ratio respectively for porous layer. $W(z)$ & $W_m(z_m)$ are the vertical velocities, $\theta(z)$ & $\theta_m(z_m)$ are the temperature distributions and $S(z)$ & $S_m(z_m)$ are the concentration distributions in fluid and porous layers respectively and a & a_m are the horizontal wave numbers. Since the horizontal wave numbers must be the same for the composite layers, so that we have $\frac{a}{d} = \frac{a_m}{d_m}$ and hence $a_m = \hat{d}a$, here $\hat{d} = \frac{d_m}{d}$ is the depth ratio.

3. Boundary Conditions

The following boundary conditions are used to solve the equations (21) to (26) and they are

$$D^2W(1) + M_t a^2\theta(1) + M_s a^2 S(1) = 0 \tag{27}$$

The velocity boundary conditions are

$$\begin{aligned}
&W(1) = 0, W_m(-1) = 0, D_m W_m(-1) = 0, \hat{T}W(0) = W_m(0),\\
&\text{当} \hat{T}d^2(D^2 + a^2)W(0) = \hat{\mu}(D_m^2 + a_m^2)W_m(0), Td\hat{D}W(0) = D_m W_m(0),\\
&\hat{T}d^3\beta^2[(D^3 - 3a^2 D)]W(0) = [-D_m + \hat{\mu}\beta^2(D_m^3 - 3a_m^2 D_m)]W_m(0)
\end{aligned} \tag{28}$$

The temperature distribution boundary conditions are

$$D\theta(1) = 0, \theta(0) = \hat{T}\theta_m(0), D\theta(0) = D_m\theta_m(0), \theta_m(-1) = 0 \tag{29}$$

The salinity distribution boundary conditions are

$$DS(1) = 0, S(0) = \hat{S}S_m(0), DS(0) = D_m S_m(0), D_m S_m(-1) = 0 \tag{30}$$

In the above equations, $\hat{S} = \frac{C_l - C_0}{C_0 - C_u}$ is the solute diffusivity ratio, $\hat{T} = \frac{T_l - T_0}{T_0 - T_u}$ is the thermal ratio, $M_t = -\frac{\partial\sigma_t}{\partial T}\frac{(T_0 - T_u)d}{\mu\kappa}$ is the thermal Marangoni number , $M_s = -\frac{\partial\sigma_t}{\partial C}\frac{(C_0 - C_u)d}{\mu\kappa}$ is the solute Marangoni number and σ_t is the surface tension.

4. Solution Methodology

The system of equations (21)-(26) are solved by using exact technique. The solutions of $W(z)$ and $W_m(z_m)$ are obtained by solving (21) and (24) using the velocity boundary conditions (28), as follows

$$W(z) = A_1[\cosh \delta z + a_1 \sinh \delta z + a_2 \cosh \zeta z + a_3 \sinh \zeta z] \quad (31)$$

$$W_m(z_m) = A_1[a_4 \cosh \eta_m z_m + a_5 \sinh \eta_m z_m + a_6 \cosh \psi_m z_m + a_7 \sinh \psi_m z_m] \quad (32)$$

where

$$\delta = \frac{\sqrt{Q} + \sqrt{Q + 4a^2}}{2}, \zeta = \frac{\sqrt{Q} - \sqrt{Q + 4a^2}}{2}, \eta_m = \sqrt{\frac{E + \sqrt{E^2 - 4F}}{2}}, \psi_m = \sqrt{\frac{E - \sqrt{E^2 - 4F}}{2}},$$

$$E = \frac{(2\mu\beta^2 a_m^2 + 1 + Q_m \beta^2)}{\mu\beta^2}, F = \frac{(a_m^2 + a_m^4 \mu\beta^2)}{\mu\beta^2},$$

$$a_1 = \frac{1}{\delta_{14}}(a_6\delta_{15} + a_7\delta_{16} + \delta_{17}), a_2 = a_6\delta_5 + \delta_6, a_3 = \frac{1}{\delta_9}(a_1\delta_{10} + a_7\delta_{11}),$$

$$a_4 = \delta_7 + a_6\delta_8, a_5 = a_1\delta_{12} + a_7\delta_{13}, a_6 = \frac{\delta_{23}\delta_{25} - \delta_{26}\delta_{22}}{\delta_{25}\delta_{21} - \delta_{24}\delta_{22}},$$

$$a_7 = \frac{\delta_{23}\delta_{24} - \delta_{26}\delta_{21}}{\delta_{24}\delta_{22} - \delta_{25}\delta_{21}}, \delta_1 = T\beta^2 d^3(\delta^3 - 3a^2\delta), \delta_2 = T\beta^2 d^3(\zeta^3 - 3a^2\zeta),$$

$$\delta_3 = \mu\beta^2(\eta_m^3 - 3a_m^2\eta_m) - \eta_m, \delta_4 = \mu\beta^2(\psi_m^3 - 3a_m^2\psi_m) - \psi_m,$$

$$\delta_5 = \frac{\hat{\mu}[(\psi_m^2 + a_m^2) - \hat{T}(\eta_m^2 + a_m^2)]}{[T\hat{d}^2(\zeta^2 + a^2) - \hat{\mu}T(\eta_m^2 + a_m^2)]}, \qquad \delta_6 = \frac{[\hat{\mu}(\eta_m^2 + a_m^2) - d^2(\delta^2 + a^2)]}{[d^2(\zeta^2 + a^2) - \hat{\mu}(\eta_m^2 + a_m^2)]},$$

$$\delta_7 = T(1 + \delta_6), \delta_8 = T\delta_5 - 1, \delta_9 = \delta_2 - \frac{T\hat{d}\zeta\delta_3}{\eta_m}, \delta_{10} = -\delta_1 + \frac{Td\delta\delta_3}{\eta_m},$$

$$\delta_{11} = \delta_4 - \frac{\psi\delta_3}{\eta_m}, \delta_{12} = \frac{1}{\eta_m}(\hat{T}\hat{d}\delta + \frac{\zeta\delta_{10}}{\delta_9}), \delta_{13} = \frac{1}{\eta_m}[(\frac{\hat{T}\hat{d}\zeta\delta_{11}}{\delta_9} - \psi_m)],$$

$$\delta_{14} = \sinh\delta + \frac{\delta_{10}\sinh\zeta}{\delta_9}, \delta_{15} = \delta_5\cosh\zeta, \delta_{16} = \frac{\delta_{11}\sinh\zeta}{\delta_9},$$

$$\delta_{17} = \delta_6\cosh\zeta + \cosh\delta, \delta_{18} = \frac{\delta_{12}\delta_{15}}{\delta_{14}}, \delta_{19} = \frac{\delta_{12}\delta_{16}}{\delta_{14}} + \delta_{13}, \delta_{20} = \frac{\delta_{12}\delta_{17}}{\delta_{14}},$$

$$\delta_{21} = \delta_8\cosh\eta_m - \delta_{18}\sinh\eta_m + \cosh\psi_m,$$

$$\delta_{22} = -\delta_{19}\sinh\eta_m - \sinh\psi_m, \delta_{23} = \delta_{20}\sinh\eta_m - \delta_7\cosh\eta_m,$$

$$\delta_{24} = -\eta_m\delta_8\sinh\eta_m - \delta_{18}\eta_m\cosh\eta_m - \psi_m\sinh\psi_m, \qquad \delta_{25} = -\eta_m\delta_{19}\cosh\eta_m + \psi_m\cosh\psi_m,$$

$$\delta_{26} = \delta_{20}\eta_m\cosh\eta_m + \delta_7\eta_m\sinh\eta_m$$

Solving equations (23) and (26) for the salinity distributions $S(z)$ and $S_m(z_m)$ using the following salinity/concentration boundary condition (30), as follows

$$S(z) = A_1[c_{13}\cosh az + c_{14}\sinh az + f_1(z)] \quad (33)$$

$$S_m(z_m) = A_1[c_{15}\cosh a_m z_m + c_{16}\sinh a_m z_m + f_{m1}(z_m)] \quad (34)$$

Where $f_1(z)=\frac{-1}{\tau}[\frac{\cosh\delta z+a_1\sinh\delta z}{\delta^2-a^2}+\frac{a_2\cosh\zeta z+a_3\sinh\zeta z}{\zeta^2-a^2}]$

$f_{m1}(z_m)=\frac{-1}{\tau_{pm}}[\frac{a_4\cosh\eta_m z_m+a_5\sinh\eta_m z_m}{\eta_m^2-a_m^2}+\frac{a_6\cosh\psi_m z_m+a_7\sinh\psi_m z_m}{\psi_m^2-a_m^2}]$

$c_{13}=\hat{S}c_{15}+\Delta_{100}+\Delta_{101}, c_{14}=\frac{1}{a}(c_{16}a_m+\Delta_{102}+\Delta_{103}),$

$c_{15}=\frac{\Delta_{108}a_m\cosh a_m-\Delta_{107}\Delta_{105}}{a_m\sinh a_m\Delta_{107}+\Delta_{106}a_m\cosh a_m}$, $c_{16}=\frac{\Delta_{105}\Delta_{106}+a_m\sinh a_m\Delta_{108}}{a_m\sinh a_m\Delta_{107}+\Delta_{106}a_m\cosh a_m}$

$\Delta_{100}=\frac{-\hat{S}}{\tau_{pm}}[\frac{a_4}{\eta_m^2-a_m^2}+\frac{a_6}{\psi_m^2-a_m^2}], \Delta_{101}=\frac{1}{\tau}[\frac{1}{\delta^2-a^2}+\frac{a_2}{\zeta^2-a^2}]$

$\Delta_{102}=\frac{-1}{\tau_{pm}}[\frac{\eta_m a_5}{\eta_m^2-a_m^2}+\frac{\psi_m a_7}{\psi_m^2-a_m^2}], \Delta_{103}=\frac{1}{\tau}[\frac{a_1\delta}{\delta^2-a^2}+\frac{a_3\zeta}{\zeta^2-a^2}],$

$\Delta_{104}=\frac{1}{\tau}[\frac{(\sinh\delta+a_1\cosh\delta)\delta}{\delta^2-a^2}+\frac{(a_2\sinh\zeta+a_3\cosh\zeta)\zeta}{\zeta^2-a^2}],$

$\Delta_{105}=\frac{1}{\tau_{pm}}[\frac{\eta_m(-a_4\sinh\eta_m+a_5\cosh\eta_m)}{\eta_m^2-a_m^2}+\frac{\psi_m(-a_6\sinh\psi_m+a_7\cosh\psi_m)}{\psi_m^2-a_m^2}],$

$\Delta_{106}=\hat{S}a\sinh a, \Delta_{107}=a_m\cosh a,\ \Delta_{108}=\Delta_{104}-(\Delta_{100}+\Delta_{101})a\sinh a-(\Delta_{102}+\Delta_{103})\cosh a$

4.1 Case (i): Linear temperature profile

Consider the linear profile,

$f(z)=1$ and $f_m(z_m)=1$ (35)

Substituting (35) into (22) and (25), the temperature distributions $\theta(z)$ and $\theta_m(z_m)$ are obtained using the temperature boundary condition (29), as follows

$\theta(z)=A_1[c_1\cosh az+c_2\sinh az+g_1(z)]$ (36)

$\theta_m(z_m)=A_1[c_3\cosh a_m z_m+c_4\sinh a_m z_m+g_{m1}(z_m)]$ (37)

where $g_1(z)=A_1[\delta_{27}-\delta_{28}+\delta_{29}-\delta_{30}],\ g_{m1}(z_m)=A_1[\delta_{31}-\delta_{32}+\delta_{33}-\delta_{34}]$

$\delta_{27}=\frac{(E_2z+E_1)}{(\delta^2-a^2)}(\cosh\delta z+a_1\sinh\delta z), \delta_{28}=\frac{2\delta E_2}{(\delta^2-a^2)^2}(a_1\cosh\delta z+\sinh\delta z)$

$\delta_{29}=\frac{(E_2z+E_1)}{(\zeta^2-a^2)}(a_2\cosh\zeta z+a_3\sinh\zeta z), \delta_{30}=\frac{2\zeta E_2}{(\zeta^2-a^2)^2}(a_3\cosh\zeta z+a_2\sinh\zeta z)$

$\delta_{31}=\frac{(E_{2m}z_m+E_{1m})}{(\eta_m^2-a_m^2)}(a_4\cosh\eta_m z_m+a_5\sinh\eta_m z_m)$

$\delta_{32}=\frac{2\eta_m E_{2m}}{(\eta_m^2-a_m^2)^2}(a_5\cosh\eta_m z_m+a_4\sinh\eta_m z_m)$

$\delta_{33}=\frac{(E_{2m}z_m+E_{1m})}{(\psi_m^2-a_m^2)}(a_6\cosh\psi_m z_m+a_7\sinh\psi_m z_m)$

$$\delta_{34} = \frac{2\psi_m E_{2m}}{(\psi_m^2 - a_m^2)^2}(a_7 \cosh \psi_m z_m + a_6 \sinh \psi_m z_m)$$

$$E_1 = R_I^* - 1, E_2 = -2R_I^*, E_{1m} = -(R_{Im}^* + 1), E_{2m} = -2R_{Im}^*\ c_1 = c_3\hat{T} + \Delta_2 - \Delta_3, c_2 = \frac{1}{a}(c_4 a_m + \Delta_4 - \Delta_5),$$

$$c_3 = \frac{\Delta_8\Delta_{10} - \Delta_{11}\Delta_6}{-\Delta_7\Delta_{10} - \Delta_9\Delta_6}, c_4 = \frac{\Delta_8\Delta_9 + \Delta_{11}\Delta_7}{\Delta_6\Delta_9 + \Delta_{10}\Delta_7},\ \Delta_1 = -[\delta_{35} + \delta_{36} + \delta_{37} + \delta_{38}],$$

$$\delta_{35} = \frac{\delta(E_2 + E_1)}{(\delta^2 - a^2)}(a_1 \cosh \delta + \sinh \delta),\ \delta_{36} = [\frac{E_2}{(\delta^2 - a^2)} - \frac{2\delta^2 E_2}{(\delta^2 - a^2)^2}](\cosh \delta + a_1 \sinh \delta),$$

$$\delta_{37} = \frac{\zeta(E_2 + E_1)}{(\zeta^2 - a^2)}(a_3 \cosh \zeta + a_2 \sinh \zeta),\ \delta_{38} = [\frac{E_2}{(\zeta^2 - a^2)} - \frac{2\zeta^2 E_2}{(\zeta^2 - a^2)^2}](a_2 \cosh \zeta + a_3 \sinh \zeta),$$

$$\Delta_2 = \hat{T}[\frac{E_{1m}a_4}{(\eta_m^2 - a_m^2)} - \frac{2E_{2m}\eta_m a_5}{(\eta_m^2 - a_m^2)^2} + \frac{E_{1m}a_6}{(\psi_m^2 - a_m^2)} - \frac{2E_{2m}\psi_m a_7}{(\psi_m^2 - a_m^2)^2}],$$

$$\Delta_3 = \frac{E_1}{(\delta^2 - a^2)} - \frac{2\delta a_1 E_2}{(\delta^2 - a^2)^2} + \frac{a_2 E_1}{(\zeta^2 - a^2)} - \frac{2\zeta a_3 E_2}{(\zeta^2 - a^2)^2},$$

$$\Delta_4 = [\frac{E_{2m}}{(\eta_m^2 - a_m^2)} - \frac{2\eta_m^2 E_{2m}}{(\eta_m^2 - a_m^2)^2}]a_4 + \frac{\eta_m a_5 E_{1m}}{(\eta_m^2 - a_m^2)} + \delta_{42}\ \delta_{42} = [\frac{E_{2m}}{(\psi_m^2 - a_m^2)} - \frac{2\psi_m^2 E_{2m}}{(\psi_m^2 - a_m^2)^2}]a_6 + \frac{\psi_m a_7 E_{1m}}{(\psi_m^2 - a_m^2)}$$

$$\Delta_5 = \frac{E_1\delta a_1 + E_2}{(\delta^2 - a^2)} - \frac{2E_2\delta^2}{(\delta^2 - a^2)^2} + \frac{E_1\zeta a_3 + E_2 a_2}{(\zeta^2 - a^2)} - \frac{2a_2 E_2\zeta^2}{(\zeta^2 - a^2)^2},\ \Delta_6 = a_m \cosh a_m, \Delta_7 = a_m \sinh a_m,$$

$$\Delta_8 = -[\delta_{39} + \delta_{40} + \delta_{41} + \delta_{42}]\ \delta_{39} = [\frac{E_{2m}}{(\eta_m^2 - a_m^2)} - \frac{2\eta_m^2 E_{2m}}{(\eta_m^2 - a_m^2)^2}](a_4 \cosh \eta_m - a_5 \sinh \eta_m)$$

$$\delta_{40} = \eta_m \frac{(E_{1m} - E_{2m})}{(\eta_m^2 - a_m^2)}(a_5 \cosh \eta_m - a_4 \sinh \eta_m)$$

$$\delta_{40} = [\frac{E_{2m}}{(\psi_m^2 - a_m^2)} - \frac{2\psi_m^2 E_{2m}}{(\psi_m^2 - a_m^2)^2}](a_6 \cosh \psi_m - a_7 \sinh \psi_m)$$

$$\delta_{41} = \psi_m \frac{(E_{1m} - E_{2m})}{(\psi_m^2 - a_m^2)}(a_7 \cosh \psi_m - a_6 \sinh \psi_m)\ \Delta_9 = \hat{T}a \sinh a, \Delta_{10} = a_m \cosh a,$$

$$\Delta_{11} = \Delta_1 - a(\Delta_2 - \Delta_3)\sinh a - (\Delta_4 - \Delta_5)\cosh a$$

From the boundary condition (27), we have

$$M_t = -\frac{D^2 W(1) + M_s a^2 S(1)}{a^2 \theta(1)}$$

The thermal Marangoni number for the linear temperature profile is as follows

$$M_{t1} = -\frac{[\delta^2(\cosh \delta + a_1 \sinh \delta) + \zeta^2(a_2 \cosh \zeta + a_3 \sinh \zeta)]}{a^2(c_1 \cosh a + c_2 \sinh a + \Lambda_1 + \Lambda_2)} \tag{38}$$

where $\Lambda_1 = \frac{(E_2 + E_1)}{(\delta^2 - a^2)}(\cosh \delta + a_1 \sinh \delta) - \frac{2\delta E_2}{(\delta^2 - a^2)^2}(a_1 \cosh \delta + \sinh \delta)$

$$\Lambda_2 = \frac{(E_2 + E_1)}{(\zeta^2 - a^2)}(a_2 \cosh \zeta + a_3 \sinh \zeta) - \frac{2\zeta E_2}{(\zeta^2 - a^2)^2}(a_3 \cosh \zeta + a_2 \sinh \zeta)$$

4.2 Case (ii): Parabolic temperature profile

For the parabolic temperature profile,

$$f(z) = 2z \text{ and } f_m(z_m) = 2z_m \tag{39}$$

Substituting (39) into (22) and (25), the temperature distributions $\theta(z)$ and $\theta_m(z_m)$ are obtained using the temperature boundary condition (29), as follows

$$\theta(z) = A_1[c_5 \cosh az + c_6 \sinh az + g_2(z)] \tag{40}$$

$$\theta_m(z_m) = A_1[c_7 \cosh a_m z_m + c_8 \sinh a_m z_m + g_{m2}(z_m)] \tag{41}$$

where $g_2(z) = A_1[\delta_{43} - \delta_{44} + \delta_{45} - \delta_{46}], g_{m2}(z_m) = A_1[\delta_{47} - \delta_{48} + \delta_{49} - \delta_{50}]$

$$\delta_{43} = \frac{(E_4 z + E_3)}{(\delta^2 - a^2)}(\cosh \delta z + a_1 \sinh \delta z), \delta_{44} = \frac{2\delta E_4}{(\delta^2 - a^2)^2}(a_1 \cosh \delta z + \sinh \delta z)$$

$$\delta_{45} = \frac{(E_4 z + E_3)}{(\zeta^2 - a^2)}(a_2 \cosh \zeta z + a_3 \sinh \zeta z), \delta_{46} = \frac{2\zeta E_4}{(\zeta^2 - a^2)^2}(a_3 \cosh \zeta z + a_2 \sinh \zeta z)$$

$$\delta_{47} = \frac{(E_{4m} z_m + E_{3m})}{(\eta_m^2 - a_m^2)}(a_4 \cosh \eta_m z_m + a_5 \sinh \eta_m z_m)$$

$$\delta_{48} = \frac{2\eta_m E_{4m}}{(\eta_m^2 - a_m^2)^2}(a_5 \cosh \eta_m z_m + a_4 \sinh \eta_m z_m)$$

$$\delta_{49} = \frac{(E_{4m} z_m + E_{3m})}{(\psi_m^2 - a_m^2)}(a_6 \cosh \psi_m z_m + a_7 \sinh \psi_m z_m)$$

$$\delta_{50} = \frac{2\psi_m E_{4m}}{(\psi_m^2 - a_m^2)^2}(a_7 \cosh \psi_m z_m + a_6 \sinh \psi_m z_m)$$

$$E_3 = R_I^*, E_4 = -2(R_I^* + 1), E_{3m} = -R_{Im}^*, E_{4m} = -2(R_{Im}^* + 1)$$

$$c_5 = c_7 \hat{T} + \Delta_{13} - \Delta_{14}, c_6 = \frac{1}{a}(c_8 a_m + \Delta_{15} - \Delta_{16}),$$

$$c_7 = \frac{\Delta_{19}\Delta_{20} - \Delta_{22}\Delta_{17}}{-\Delta_{18}\Delta_{20} - \Delta_{21}\Delta_{17}}, c_8 = \frac{\Delta_{19}\Delta_{21} + \Delta_{22}\Delta_{18}}{\Delta_{17}\Delta_{21} + \Delta_{20}\Delta_{18}},$$

$$\Delta_{12} = -[\delta_{51} + \delta_{52} + \delta_{53} + \delta_{54}], \qquad \delta_{51} = \frac{\delta(E_4 + E_3)}{(\delta^2 - a^2)}(a_1 \cosh \delta + \sinh \delta),$$

$$\delta_{52} = [\frac{E_4}{(\delta^2 - a^2)} - \frac{2\delta^2 E_4}{(\delta^2 - a^2)^2}](\cosh \delta + a_1 \sinh \delta),$$

$$\delta_{53} = \frac{\zeta(E_4 + E_3)}{(\zeta^2 - a^2)}(a_3 \cosh \zeta + a_2 \sinh \zeta),$$

$$\delta_{54} = [\frac{E_4}{(\zeta^2 - a^2)} - \frac{2\zeta^2 E_4}{(\zeta^2 - a^2)^2}](a_2 \cosh \zeta + a_3 \sinh \zeta),$$

$$\Delta_{13} = \hat{T}[\frac{E_{3m} a_4}{(\eta_m^2 - a_m^2)} - \frac{2E_{4m}\eta_m a_5}{(\eta_m^2 - a_m^2)^2} + \frac{E_{3m} a_6}{(\psi_m^2 - a_m^2)} - \frac{2E_{4m}\psi_m a_7}{(\psi_m^2 - a_m^2)^2}],$$

$$\Delta_{14} = \frac{E_3}{(\delta^2 - a^2)} - \frac{2\delta a_1 E_4}{(\delta^2 - a^2)^2} + \frac{a_2 E_3}{(\zeta^2 - a^2)} - \frac{2\zeta a_3 E_4}{(\zeta^2 - a^2)^2},$$

$$\Delta_{15}=[\frac{E_{4m}}{(\eta_m^2-a_m^2)}-\frac{2\eta_m^2E_{4m}}{(\eta_m^2-a_m^2)^2}]a_4+\frac{\eta_m a_5E_{3m}}{(\eta_m^2-a_m^2)}+\Delta_{150}$$

$$\Delta_{150}=[\frac{E_{4m}}{(\psi_m^2-a_m^2)}-\frac{2\psi_m^2E_{4m}}{(\psi_m^2-a_m^2)^2}]a_6+\frac{\psi_m a_7E_{3m}}{(\psi_m^2-a_m^2)}$$

$$\Delta_{16}=\frac{E_3\delta a_1+E_4}{(\delta^2-a^2)}-\frac{2E_4\delta^2}{(\delta^2-a^2)^2}+\frac{E_3\zeta a_3+E_4a_2}{(\zeta^2-a^2)}-\frac{2a_2E_4\zeta^2}{(\zeta^2-a^2)^2},$$

$$\Delta_{17}=a_m\cosh a_m,\Delta_{18}=a_m\sinh a_m,\ \Delta_{19}=-[\delta_{55}+\delta_{56}+\delta_{57}+\delta_{58}]$$

$$\delta_{55}=[\frac{E_{4m}}{(\eta_m^2-a_m^2)}-\frac{2\eta_m^2E_{4m}}{(\eta_m^2-a_m^2)^2}](a_4\cosh\eta_m-a_5\sinh\eta_m)$$

$$\delta_{56}=\eta_m\frac{(E_{3m}-E_{4m})}{(\eta_m^2-a_m^2)}(a_5\cosh\eta_m-a_4\sinh\eta_m)$$

$$\delta_{57}=[\frac{E_{4m}}{(\psi_m^2-a_m^2)}-\frac{2\psi_m^2E_{4m}}{(\psi_m^2-a_m^2)^2}](a_6\cosh\psi_m-a_7\sinh\psi_m)$$

$$\delta_{58}=\psi_m\frac{(E_{3m}-E_{4m})}{(\psi_m^2-a_m^2)}(a_7\cosh\psi_m-a_6\sinh\psi_m),\Delta_{20}=\hat{T}a\sinh a,\Delta_{21}=a_m\cosh a,$$

$$\Delta_{22}=\Delta_{12}-a(\Delta_{13}-\Delta_{14})\sinh a-(\Delta_{15}-\Delta_{16})\cosh a$$

From the boundary condition (27), the thermal Marangoni number for parabolic temperature profile is as follows

$$M_{t2}=-\frac{[\delta^2(\cosh\delta+a_1\sinh\delta)+\zeta^2(a_2\cosh\zeta+a_3\sinh\zeta)]}{a^2(c_5\cosh a+c_6\sinh a+\Lambda_3+\Lambda_4)} \tag{42}$$

where $\Lambda_3=\frac{(E_4+E_3)}{(\delta^2-a^2)}(\cosh\delta+a_1\sinh\delta)-\frac{2\delta E_4}{(\delta^2-a^2)^2}(a_1\cosh\delta+\sinh\delta)$

$$\Lambda_4=\frac{(E_4+E_3)}{(\zeta^2-a^2)}(a_2\cosh\zeta+a_3\sinh\zeta)-\frac{2\zeta E_4}{(\zeta^2-a^2)^2}(a_3\cosh\zeta+a_2\sinh\zeta)$$

4.3 Case (iii): Inverted parabolic temperature profile

Consider inverted parabolic profile as

$$f(z)=2(1-z)\ \text{ and }\ f_m(z_m)=2(1-z_m) \tag{43}$$

Substituting (43) into (22) and (25), the temperature distributions $\theta(z)$ and $\theta_m(z_m)$ are obtained using the temperature boundary condition (29), as follows

$$\theta(z)=A_1[c_9\cosh az+c_{10}\sinh az+g_3(z)] \tag{44}$$

$$\theta_m(z_m)=A_1[c_{11}\cosh a_mz_m+c_{12}\sinh a_mz_m+g_{m3}(z_m)] \tag{45}$$

where $g_3(z)=A_1[\delta_{59}-\delta_{60}+\delta_{61}-\delta_{62}],g_{m3}(z_m)=A_1[\delta_{63}-\delta_{64}+\delta_{65}-\delta_{66}]$

$$\delta_{59}=\frac{(E_6z+E_5)}{(\delta^2-a^2)}(\cosh\delta z+a_1\sinh\delta z)\ \delta_{60}=\frac{2\delta E_6}{(\delta^2-a^2)^2}(a_1\cosh\delta z+\sinh\delta z)$$

$$\delta_{61}=\frac{(E_6z+E_5)}{(\zeta^2-a^2)}(a_2\cosh\zeta z+a_3\sinh\zeta z)\ \delta_{62}=\frac{2\zeta E_6}{(\zeta^2-a^2)^2}(a_3\cosh\zeta z+a_2\sinh\zeta z)$$

$$\delta_{63} = \frac{(E_{6m} z_m + E_{5m})}{(\eta_m^2 - a_m^2)} (a_4 \cosh \eta_m z_m + a_5 \sinh \eta_m z_m)$$

$$\delta_{64} = \frac{2\eta_m E_{6m}}{(\eta_m^2 - a_m^2)^2} (a_5 \cosh \eta_m z_m + a_4 \sinh \eta_m z_m)$$

$$\delta_{65} = \frac{(E_{6m} z_m + E_{5m})}{(\psi_m^2 - a_m^2)} (a_6 \cosh \psi_m z_m + a_7 \sinh \psi_m z_m)$$

$$\delta_{66} = \frac{2\psi_m E_{6m}}{(\psi_m^2 - a_m^2)^2} (a_7 \cosh \psi_m z_m + a_6 \sinh \psi_m z_m)$$

$$E_5 = R_I^* - 2, E_6 = 2(1 - R_I^*), E_{5m} = -2 - R_{Im}^*, E_{6m} = 2(1 - R_{Im}^*)$$

$$c_9 = c_{11}\hat{T} + \Delta_{24} - \Delta_{25}, c_{10} = \frac{1}{a}(c_{12} a_m + \Delta_{26} - \Delta_{27}),$$

$$c_{11} = \frac{\Delta_{30}\Delta_{31} - \Delta_{33}\Delta_{28}}{-\Delta_{29}\Delta_{31} - \Delta_{32}\Delta_{28}}, c_{12} = \frac{\Delta_{30}\Delta_{32} + \Delta_{33}\Delta_{29}}{\Delta_{28}\Delta_{32} + \Delta_{31}\Delta_{29}}, \qquad \Delta_{23} = -[\delta_{67} + \delta_{68} + \delta_{69} + \delta_{70}],$$

$$\delta_{67} = \frac{\delta(E_6 + E_5)}{(\delta^2 - a^2)} (a_1 \cosh \delta + \sinh \delta),$$

$$\delta_{68} = [\frac{E_6}{(\delta^2 - a^2)} - \frac{2\delta^2 E_6}{(\delta^2 - a^2)^2}](\cosh \delta + a_1 \sinh \delta),$$

$$\delta_{69} = \frac{\zeta(E_6 + E_5)}{(\zeta^2 - a^2)} (a_3 \cosh \zeta + a_2 \sinh \zeta),$$

$$\delta_{70} = [\frac{E_6}{(\zeta^2 - a^2)} - \frac{2\zeta^2 E_6}{(\zeta^2 - a^2)^2}](a_2 \cosh \zeta + a_3 \sinh \zeta),$$

$$\Delta_{24} = \hat{T}[\frac{E_{5m} a_4}{(\eta_m^2 - a_m^2)} - \frac{2E_{6m}\eta_m a_5}{(\eta_m^2 - a_m^2)^2} + \frac{E_{5m} a_6}{(\psi_m^2 - a_m^2)} - \frac{2E_{6m}\psi_m a_7}{(\psi_m^2 - a_m^2)^2}],$$

$$\Delta_{25} = \frac{E_5}{(\delta^2 - a^2)} - \frac{2\delta a_1 E_6}{(\delta^2 - a^2)^2} + \frac{a_2 E_5}{(\zeta^2 - a^2)} - \frac{2\zeta a_3 E_6}{(\zeta^2 - a^2)^2},$$

$$\Delta_{26} = [\frac{E_{6m}}{(\eta_m^2 - a_m^2)} - \frac{2\eta_m^2 E_{6m}}{(\eta_m^2 - a_m^2)^2}] a_4 + \frac{\eta_m a_5 E_{5m}}{(\eta_m^2 - a_m^2)} + \Delta_{260}$$

$$\Delta_{260} = [\frac{E_{6m}}{(\psi_m^2 - a_m^2)} - \frac{2\psi_m^2 E_{6m}}{(\psi_m^2 - a_m^2)^2}] a_6 + \frac{\psi_m a_7 E_{5m}}{(\psi_m^2 - a_m^2)}$$

$$\Delta_{27} = \frac{E_5 \delta a_1 + E_6}{(\delta^2 - a^2)} - \frac{2E_6 \delta^2}{(\delta^2 - a^2)^2} + \frac{E_5 \zeta a_3 + E_6 a_2}{(\zeta^2 - a^2)} - \frac{2a_2 E_6 \zeta^2}{(\zeta^2 - a^2)^2},$$

$$\Delta_{28} = a_m \cosh a_m, \Delta_{29} = a_m \sinh a_m, \qquad \Delta_{30} = -[\delta_{71} + \delta_{72} + \delta_{73} + \delta_{74}]$$

$$\delta_{71} = [\frac{E_{6m}}{(\eta_m^2 - a_m^2)} - \frac{2\eta_m^2 E_{6m}}{(\eta_m^2 - a_m^2)^2}](a_4 \cosh \eta_m - a_5 \sinh \eta_m)$$

$$\delta_{72} = \eta_m \frac{(E_{5m} - E_{6m})}{(\eta_m^2 - a_m^2)} (a_5 \cosh \eta_m - a_4 \sinh \eta_m)$$

$$\delta_{73} = [\frac{E_{6m}}{(\psi_m^2 - a_m^2)} - \frac{2\psi_m^2 E_{6m}}{(\psi_m^2 - a_m^2)^2}](a_6 \cosh \psi_m - a_7 \sinh \psi_m)$$

$$\delta_{74} = \psi_m \frac{(E_{5m} - E_{6m})}{(\psi_m^2 - a_m^2)}(a_7 \cosh \psi_m - a_6 \sinh \psi_m) \qquad \Delta_{31} = \hat{T}a \sinh a, \Delta_{32} = a_m \cosh a,$$

$$\Delta_{33} = \Delta_{23} - a(\Delta_{24} - \Delta_{25}) \sinh a - (\Delta_{26} - \Delta_{27}) \cosh a$$

From the boundary condition (27), the thermal Marangoni number for inverted parabolic temperature profile is as follows

$$M_{t3} = -\frac{[\delta^2(\cosh \delta + a_1 \sinh \delta) + \zeta^2(a_2 \cosh \zeta + a_3 \sinh \zeta)]}{a^2(c_9 \cosh a + c_{10} \sinh a + \Lambda_5 + \Lambda_6)} \tag{46}$$

where $\Lambda_5 = \frac{(E_6 + E_5)}{(\delta^2 - a^2)}(\cosh \delta + a_1 \sinh \delta) - \frac{2\delta E_6}{(\delta^2 - a^2)^2}(a_1 \cosh \delta + \sinh \delta)$

$\Lambda_6 = \frac{(E_6 + E_5)}{(\zeta^2 - a^2)}(a_2 \cosh \zeta + a_3 \sinh \zeta) - \frac{2\zeta E_6}{(\zeta^2 - a^2)^2}(a_3 \cosh \zeta + a_2 \sinh \zeta)$.

5. Results and Discussion

The present study primarily focuses on the combined effects of nonuniform temperature gradients and heat source on double diffusive Bènard-Marangoni convection in a porous-fluid system in the presence of vertical magnetic field. The results as a whole, is not comparable with the bench mark solutions. But it is comparable, qualitatively in the limiting case. As $\hat{d} \to 0$ i.e., $d_m \to 0$ i.e., single fluid layer and $\hat{d} \to \infty$ i.e., $d \to 0$ i.e., single porous layer, the present results match qualitatively with the corresponding earlier works [21-24]. The effects of porous parameter β, Chandrasekhar number Q, viscosity ratio $\hat{\mu}$, modified internal Rayleigh numbers R_I^* and R_{Im}^* for fluid and porous region, solute Marangoni number M_s, diffusivity ratios τ and τ_{pm} in fluid and porous region and different temperature gradients on the linear stability of double diffusive Bènard-Marangoni convection in a porous-fluid system in the presence of vertical magnetic field effect is investigated with the aim of controlling the convection. The resulting Eigen value is solved exactly and the expression for Marangoni number is obtained. Thermal Marangoni numbers M_{t1}, M_{t3}, M_{t3} for linear, parabolic and inverted parabolic temperature profiles, respectively, against the thermal ratio $\hat{T}$ for the various parameters discussed above are depicted in figures 2-9 for the values of $a = 2.5, \hat{d} = 0.2, \beta = 1.0,$ $\hat{\mu} = 2,$ $\hat{S} = 1,$ $\tau = \tau_{pm} = 0.25,$ $Q = 10, M_s = 10, R_I^* = 1$ and $R_{Im}^* = 1$.

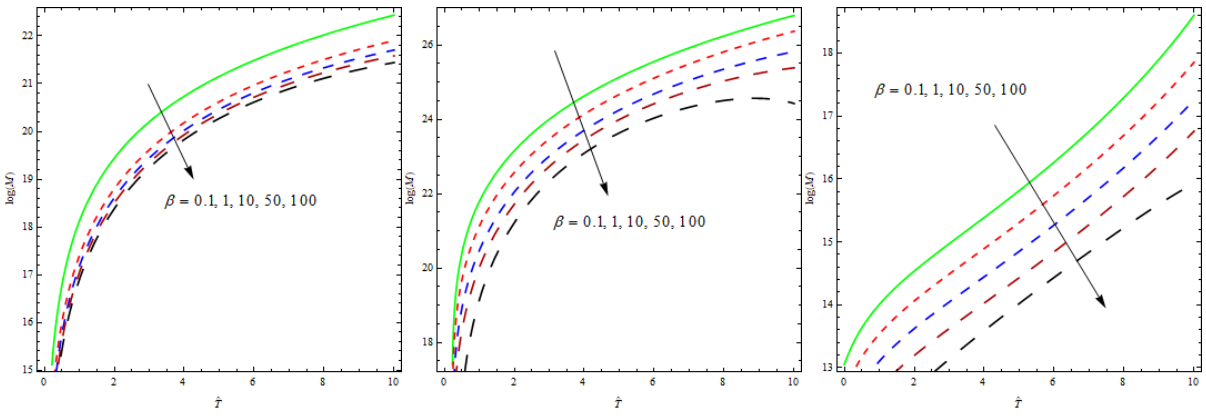

Fig.2 Effects of porous parameter β

Increase in permeability allows more fluid movement there by decreasing the surface tension. This effect can be observed in Fig. 2 which is for $\beta = 0.1,1,10,50,100$. As β increases $M(M_{t1}, M_{t3}, M_{t3})$ decrease for all the three temperature profiles. This effect is more significant for inverted parabolic temperature profile as seen in Fig. 2c. From these figures it is clear that $M_{t2}(\beta) > M_{t1}(\beta) > M_{t3}(\beta)$. As $\hat{T}$ increases, M also increases. This may be due to the fact that the temperature gradient is less in fluid region, where Marangoni convection is happening there by indicating that surface tension is comparatively more in the fluid region.

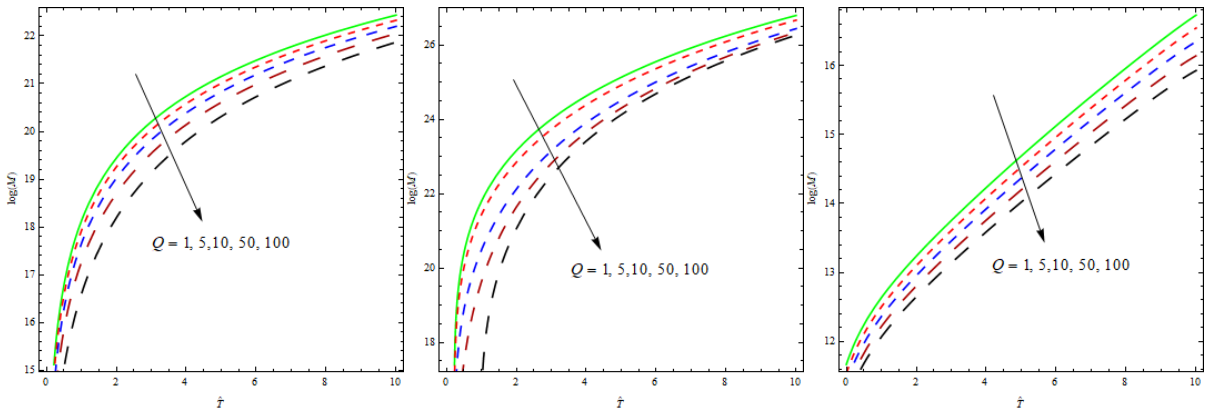

Fig.3 Effects of Chandrasekhar number Q

Increase in Q, decreases M irrespective of the temperature profiles for the values $Q = 1,5,10,50,100$. Usually the effect of Q, is to stabilize the system but the reverse is observed here. The two diffusing components acting opposite each other with heat source in the presence of magnetic field might be a region for this result. The effect of $\hat{T}$ is similar to that found in Fig. 2. Different temperature profiles have different effects on M. The curves seem to be converging for parabolic temperature profile as compared to the curves for linear and inverted parabolic temperature profiles indicating the importance of Q for wide ranging values of $\hat{T}$. From Fig. 3a, 3b, 3c one can note that $M_{t2}(Q) > M_{t1}(Q) > M_{t3}(Q)$. This implies that the strength of the magnetic field can be suitably chosen with the relevant temperature profiles to control convection.

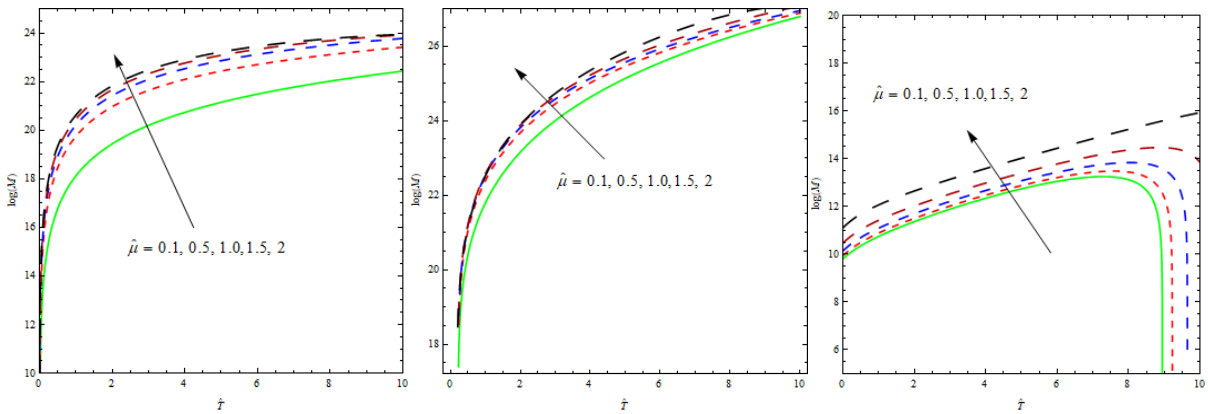

Fig.4 Effects of viscosity ratio $\hat{\mu}$

Fig. 4 is the plot of M vs. $\hat{T}$ for different values of $\hat{\mu} = 0.1, 0.5, 1, 1.5, 2$. It may be observed that the effect of $\hat{\mu}$ is to stabilize the system. Physically, as viscosity increases, the resistance to the flow increases which increases the surface tension. Once again, we see that for a given $\hat{T}$, $M_{t2}(\mu) > M_{t1}(\mu) > M_{t3}(\mu)$. Increase in $\hat{T}$ increases M for all the three profiles except that M_3 increases up to $\hat{T} \approx 8$ and then a sudden decrease. This might be due to the large temperature ratio and the nature of the temperature profile.

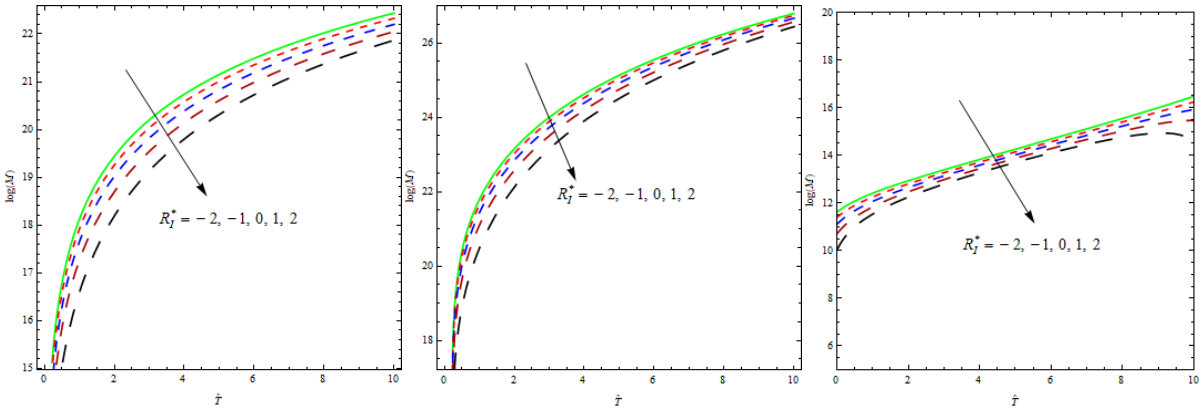

Fig.5 Effects modified internal Rayleigh number R_I^*

The effect of $R_I^* = -2, -1, 0, 1, 2$ is to decrease M for all the three profiles. As the strength of heat source increases, in the fluid region, where Marangoni convection is happening, increases the temperature which clearly decreases the surface tension there by decreasing M . This result is depicted in Fig.5. Figure 5a shows that the effect of R_I^* is prominent for linear temperature profile in comparison with the other two profiles. For a given $\hat{T}$ it is observed that $M_{t2}(R_I^*) > M_{t1}(R_I^*) > M_{t3}(R_I^*)$. The effect of $\hat{T}$ is similar to the observations recorded earlier.

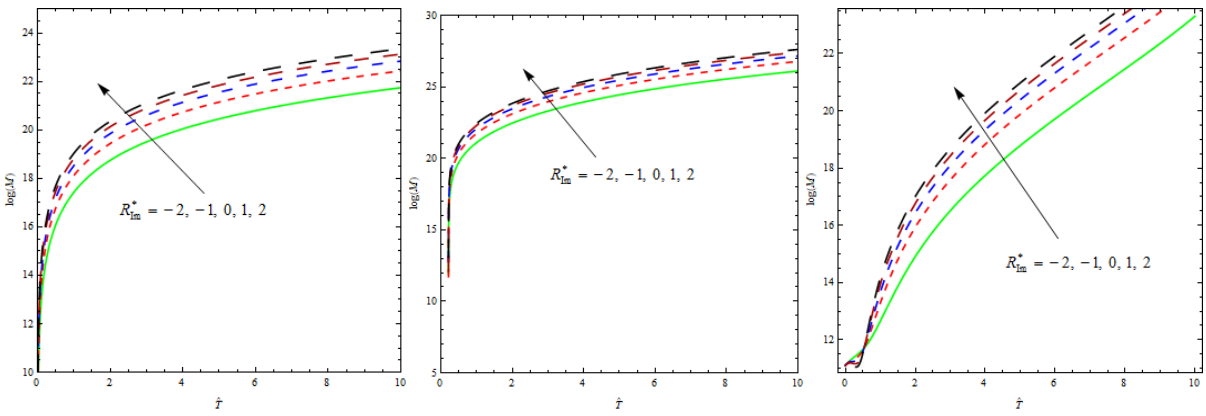

Fig.6 Effects modified internal Rayleigh number R_{Im}^* for porous region

From Fig. 6, one can see that the effect of $R_{Im}^{*}=-2,-1,0,1,2$ is opposite to that of R_{I}^{*}. These graphs clearly indicate that in the porous region, increase in the strength of source stabilizes the system as expected. It can also be noted that R_{Im}^{*} is more dominant for linear and inverted parabolic temperature profiles. The effect of $\hat{T}$ is to stabilize the system as seen in other figures.

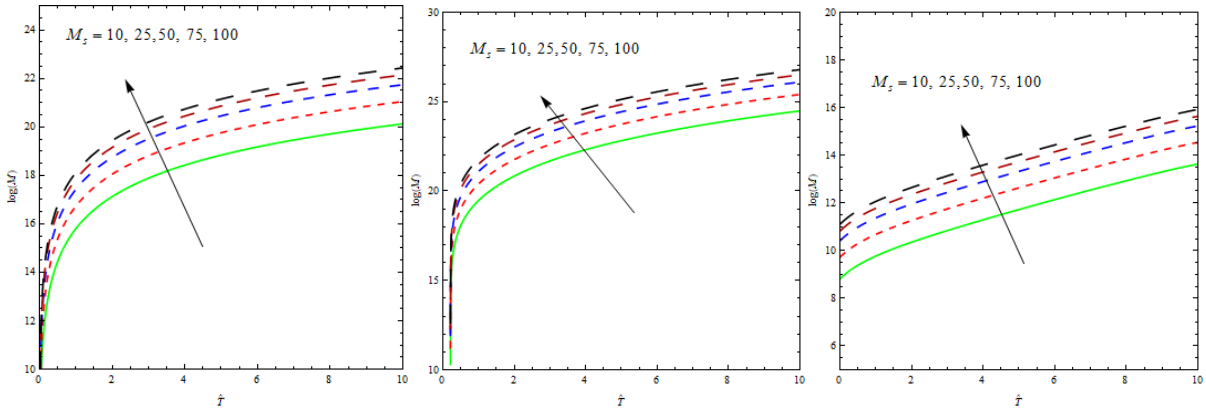

Fig.7 Effects of solute Marangoni number M_s

The effect of $M_s=10,25,50,75,100$ is qualitatively similar to the effect of R_{Im}^{*}. Physically, solutal Marangoni number stabilizes the system. We observe that from Fig. 7, the curves are more diverging for all the three profiles with increasing $\hat{T}$. Here again, for a given $\hat{T}$, $M_{t2}(M_s)>M_{t1}(M_s)>M_{t3}(M_s)$. As expected, increase in thermal ratio stabilizes the system.

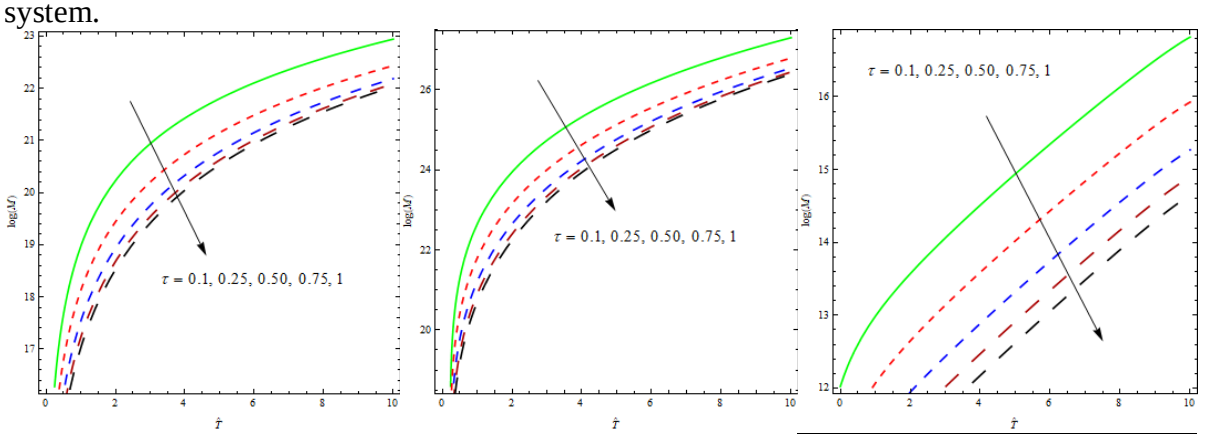

Fig.8 Effects of diffusivity ratio τ

Fig. 8 and 9 show the effect of $\tau=0.1,0.25,0.50,0.75,1$ and τ_{pm}=0.1, 0.25, 0.50, 0.75, 1 on M. Increase in τ and τ_{pm} destabilize the system there by augmenting the onset of Marangoni convection. This effect is seen for all the three profiles. The curves for the variations of τ brings in larger variations in M as compared to those of τ_{pm}. Diffusivity has a dominating effect for inverted parabolic profile indicating the choice of temperature profile

plays a crucial role in controlling the convection. The effect of τ and τ_{pm} is more stabilizing for parabolic temperature profile. Increase in $\hat{T}$ is to stabilize the system.

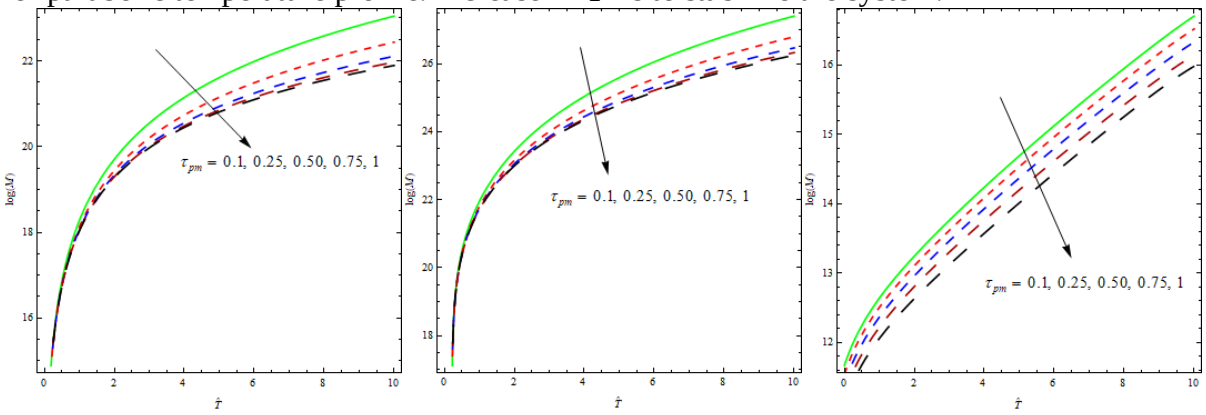

Fig.9 Effects of diffusivity ratio τ_{pm} in porous region

From Fig. 9, we also observe that for small values of $\hat{T}$, i.e., $0.2 < \hat{T} < 1$, there is no effect of τ_{pm} for linear and parabolic temperature profiles, for $\hat{T} > 1$ the curves diverges.

6. Conclusion

Some of the following conclusions are drawn from the study:

(i) The effect of Chandrasekhar number Q destabilizing the system is an unexpected result from the study. This may be due to the fact that the two diffusing components act opposite to each other with heat source in the presence of vertical magnetic field.

(ii) Lesser the thermal ratio higher the surface tension as seen in the figures (especially in the fluid region).

(iii) Larger viscosity ratio $\hat{\mu}$ stabilizes the system even when the thermal ratio increases.

(iv) The strength of heat source (sink) is so chosen that it does not induce convection by itself.

(v) Parabolic temperature profile is highly stable among the three temperature gradients.

(vi) The choice of temperature profile helps in delaying or augmenting convection.

Acknowledgement

The authors are thankful to Late Prof. N. Rudraiah and Hon. Prof. I. S. Shivakumara, Professor and Hon. Prof. P. G. Siddheshwar Professor, Department of Mathematics, Bangalore University, Bengaluru, for their help during the formulation of the problem.

References

[1] Sumithra R., Manjunatha N., An exact study of the effects of parabolic and inverted parabolic temperature gradients on surface tension driven magneto convection in a composite layer, International Journal of Recent Technology and Engineering, 3 (5) (2014) 36-46.

[2] Noureddine Hadidi, Rachid Bennacer., Yacine Ould-amer., Numerical study of double-diffusive convection developed within horizontal partially porous enclosure, Desalination and Water Treatment, 57(48-49) (2016) 23217-23224.

[3] Manjunatha N., Sumithra R., Effects of non-uniform temperature gradients on double diffusive Marangoni convection in a two layer system, International Journal of Pure and Applied Mathematics, 118(2) (2018) 203-220.

[4] Altawallbeh A A., I. Hashim, B. S. Bhadauria., Magneto-double diffusive convection in a viscoelastic fluid saturated porous layer with internal heat source, AIP Conference Proceedings 2116, 030015 (2019). https://doi.org/10.1063/1.5113999.

[5] Sumithra R , Komala B., Manjunatha N ., Darcy-Benard double diffusive Marangoni convection with Soret effect in a composite layer system, Malaya Journal of Matematik, 8(4) (2020) 1473-1479.

[6] Nor Fadzillah Mohd Mokhtar, Roslinda Nazar, Fudziah Ismail, Norihan Md Arifin, MohamedSuleiman., Marangoni convection in a fluid saturated porous layer with a deformable free surface, International Journal of Mathematical and Computational Sciences, 3(2) (2009) 137-142.

[7] Gangadharaiah Y.H., Onset of Benard–Marangoni convection in a composite layer with anisotropic porous material, Journal of Applied Fluid Mechanics, 9(3) (2016) 1551-1558.

[8] K. Mehmood, S. Hussain, and M. Sagheer., Mixed convection flow with non-uniform heat source/sink in a doubly stratified magneto nanofluid, AIP Advances, 6 (6) 065126 (2016); https://doi.org/10.1063/1.4955157.

[9] Dileep Kumar and A.K.Singh., Effects of heat source/sink and induced magnetic field on natural convective flow in vertical concentric annuli, Alexandria Engineering Journal, 55(4) (2016) 3125-3133.

[10] Sravanthi, C. S., Gorla, R. S. R., Effects of heat source/sink and chemical reaction on MHD Maxwell nanofluid flow over a convectively heated exponentially stretching sheet using Homotopy analysis method, International Journal of Applied Mechanics and Engineering, 23(1) (2018) 137-159.

[11] Upreti, H., Rawat, S.K. and Kumar, M., Radiation and non-uniform heat sink/source effects on 2D MHD flow of CNTs- H_2O nanofluid over a flat porous plate, Multidiscipline Modeling in Materials and Structures,16(4) (2019) 791-809.

[12] Nurul Hafizah Zainal Abidin, Nor Fadzillah Mohd Mokhtar, Zanariah Abdul Majid. Onset of Benard-Marangoni instabilities in a double diffusive binary fluid layer with temperature-dependent viscosity, Numerical Algebra, Control & Optimization, 9 (4) (2019) 413-421.

[13] M K Nayak, A K Abdul Hakeem and B Ganga., Influence of non-uniform heat source/sink and variable viscosity on mixed convection flow of third grade nanofluid over an inclined stretched Riga plate, International Journal of Thermofluid Science and Technology, 6 (4) (2019) 19060401.

[14] Nadeem, S., Ijaz, M., Ayub, M. Darcy-Forchheimer flow under rotating disk and entropy generation with thermal radiation and heat source/sink, J Therm. Anal. Calorim., (2020). https://doi.org/10.1007/s10973-020-09737-1.

[15] Thirupathi Thumma and S.R. Mishra., Effect of nonuniform heat source/sink, and viscous and Joule dissipation on 3D Eyring–Powell nanofluid flow over a stretching sheet, Journal of Computational Design and Engineering, 7 (2020) 1-15.

[16] Chamkha, Ali J., Yassen, Rizk., Ismael, Muneer A., Rashad, A.M., Salah, T., Nabwey, Hossam A., MHD free convection of localized heat source/sink in hybrid nanofluid-filled square cavity, Journal of Nanofluids, 9(1) (2020) 1-12.

[17] Talha Anwar, Poom Kumam, Zahir Shah, Wiboonsak Watthayu and Phatiphat Thounthong., Molecules unsteady radiative natural convective MHD nanofluid flow past a porous moving vertical plate with heat source/sink, Molecules, 25(4) (2020) 854.

[18] Mandal, I.C., Mukhopadhyay, S., Nonlinear convection in micropolar fluid flow past a non-isothermal exponentially permeable stretching sheet in presence of heat source/sink, Therm. Eng., 67 (2020) 202–215.

[19] G. Dharmaiah, O.D. Makinde, K.S. Balamurugan., Perturbation analysis of thermophoresis, hall current and heat source on flow dissipative aligned convective flow about an inclined plate, International Journal of Thermofluid Science and Technology , 7(1) (2020) 20070103.

[20] Tarikul Islam, Nazma Parveen, Md. Fayz-Al-Asad., Hydromagnetic natural convection heat transfer of Copper-Water nanofluid within a right-angled triangular cavity, International Journal of Thermofluid Science and Technology , 7(3) (2020) 070304.

[21] Manjunatha. N and Sumithra R., Effects of heat source/sink and nonuniform temperature gradients on Benard-surface tension driven convection in a composite layer in the presence of vertical magnetic field, Gedrag en Organisatie , 33(2) (2020a) 865-879.

[22] Manjunatha. N and Sumithra R., Effects of uniform and non-uniform temperature gradients on non-Darcian-Benard-magneto-Marangoni convection in composite layer in the presence of constant heat source/sink, Gedrag en Organisatie , 33(2) (2020b) 880-896.

[23] R.K. Vanishree, Sumithra R and Manjunatha N., Effect on uniform and nonuniform temperature gradients on Benard-Marangoni convection in a superposed fluid and porous layer in the presence of heat source, Gedrag en Organisatie , 33(2) (2020) 746-758.

[24] Manjunatha N., Sumithra R., Effects of non-uniform temperature gradients on surface tension driven two component magneto convection in a porous-fluid system, ARPN Journal of Engineering and Applied Sciences, 13 (2) (2018) 429-441.